ADVANCED ELECTRONIC MATERIALS
www.advelectronicmat.de

Bioinspired Electronic Whisker Arrays by Pencil-Drawn Paper for Adaptive Tactile Sensing

*Qilin Hua, Haitao Liu, Jing Zhao, Dengfeng Peng, Xiaonian Yang, Lin Gu, and Caofeng Pan**

Many mammals, e.g., cats, rats, and seals, relying on their long facial whiskers instead of their vision system, can easily find their way in narrow, dark or murky environments. The whiskers (or vibrissae) of these animals provide remarkable tactile units to sense the external environment. For example, cats are capable of discriminating all of an object's spatial properties, including size, orientation and shape, according to tactile feedback from their whiskers. Nowadays, new approaches for developing artificial electronic whiskers (e-whiskers) to mimic mammalian vibrissal tactile perception are of great importance in advanced robotics,[1–4] artificial intelligence,[5] and human-machine interfaces.[6,7] Some recent advances in piezoelectric,[8–10] resistive,[11–13] and capacitive[14,15] devices have been reported to sense tactile signals adaptively. To data, e-whiskers have been outlined with binary contact sensor, capacitor microphone sensor, force/torque sensor, strain gauge, etc.[2] Among them, e-whiskers based on highly strain-sensitive nanostructured films have been recently demonstrated the capability of sensing the environmental factors such as strain (CNT-Ag nanoparticles)[6,7] and temperature (PEDOT:PSS-CNT).[7] However, the complex fabrication process and large expenditure of these reported e-whiskers would restrict their broad applications. Hence the facile and cost-effective approaches for e-whiskers are urgent to be explored. Pencil drawn paper, known as pencil-on-paper approach, illustrates an effective way of constructing graphitic strain sensors in a solvent-free or nonvacuum manner, with high gauge factor (GF), fast response, and good durability.[12,16–20] Moreover, personalized strain sensors can be easily fabricated only with a pencil, a pair of scissors, and a piece of paper in a few minutes. In addition to multiple advantages of the fabrication methods itself, paper-based devices also exhibit many virtues of lightweight, disposable, and easily-available characteristics.[19–22] Here, we present a versatile approach to fabricate bioinspired e-whisker arrays with a superior strain sensitivity (GF = 34), fast response (50 ms), and high durability/stability by using pencil-drawn paper. It demonstrates a good performance on adaptive tactile sensing/imaging, strain monitoring, 3D spatial mapping as well as detailed objects' localization, orientation, and shape reconstruction.

Q. Hua, H. Liu, J. Zhao, Dr. D. Peng,
X. Yang, Prof. C. Pan
Beijing Institute of Nanoenergy and Nanosystems
Chinese Academy of Sciences National Center
for Nanoscience and Technology (NCNST)
Beijing 100083, P. R. China
E-mail: cfpan@binn.cas.cn
Prof. L. Gu
Institute of Physics
Chinese Academy of Sciences
P. O. Box 603, Beijing 100190, P. R. China

DOI: 10.1002/aelm.201600093

Figure 1a illustrates a cartoon cat with several long facial vibrissae drawn by a pencil. Under the inspiration of the biofunctions of vibrissae, we design a device that imitates the mammal's tactile perception to detect the environment factors. The scheme of the target device, known as e-whisker, is shown in Figure 1b, which is simply fabricated using pencil trace by a graphite pencil that drawn on a piece of paper. Figure 1c demonstrates the paper covered with graphite trace, and Figure 1d shows the corresponding SEM image. We can see that the paper covered with a large number of graphite particles in Figure 1d and Figure S1e,f of the Supporting Information. For a comparison, we investigate the morphology of a blank paper on which it shows rough and porous surface composited with a great many cellulose fibers (Figure S1a, Supporting Information). It should be noted that the special rough structure of the paper surface could facilitate the covering graphite particles and flakes. As a more specifically experimental process to cover a jointed layer of graphite, a 2B pencil is scratched on the paper forward one direction, the pencil graphite particles or flakes can be exfoliated and coated around the cellulose fibers (see Figure S1b, Supporting Information). Repeatedly, the pencil is drawn on the paper for ten time, the graphite particles or flakes are strongly adhered on the paper and form a well layer of graphite chunks with a flat surface, as shown in Figure S1c of the Supporting Information. The Raman spectrum of the pencil trace shows the characteristic peaks of graphite in Figure 1e. The spectrum shows three pronounced peaks at 1350, 1573, and ≈2700 cm^{-1} of graphite, corresponding to the D, G, and 2D bands, respectively (see Figure 1e).

The graphite pencil trace at outward and inward deflections is schematically illustrated in **Figure 2**a. It describes that the pencil trace on paper can be well conducted as a strain sensor in which resistance of the graphite varies with strains of paper deflection. Figure S2 of the Supporting Information shows changes in resistance have linear relations both with applied strains at tensile (outward) and compressive (inward) bending. The sensing properties of the sensor originate from the reversible microcontacts change in graphite flakes of the pencil-drawn paper.[13] Specifically, microcracks would appear in neighboring graphite flakes when applied a tensile strain, leading to a pronounced increase of resistance (see Figure 2b,d and Figure S2, Supporting Information); On the contrary, the neighboring graphite flakes could reconstruct overlaps when applied a compressive strain, resulting in an obvious decrease of resistance (see Figure 2c,e and Figure S2, Supporting Information). Based on strain sensing properties of the pencil-drawn paper, we design a cantilever structure using the pencil-on-paper

 © 2016 WILEY-VCH Verlag GmbH & Co. KGaA, Weinheim

ADVANCED ELECTRONIC MATERIALS
www.advelectronicmat.de

Materials Views
www.MaterialsViews.com

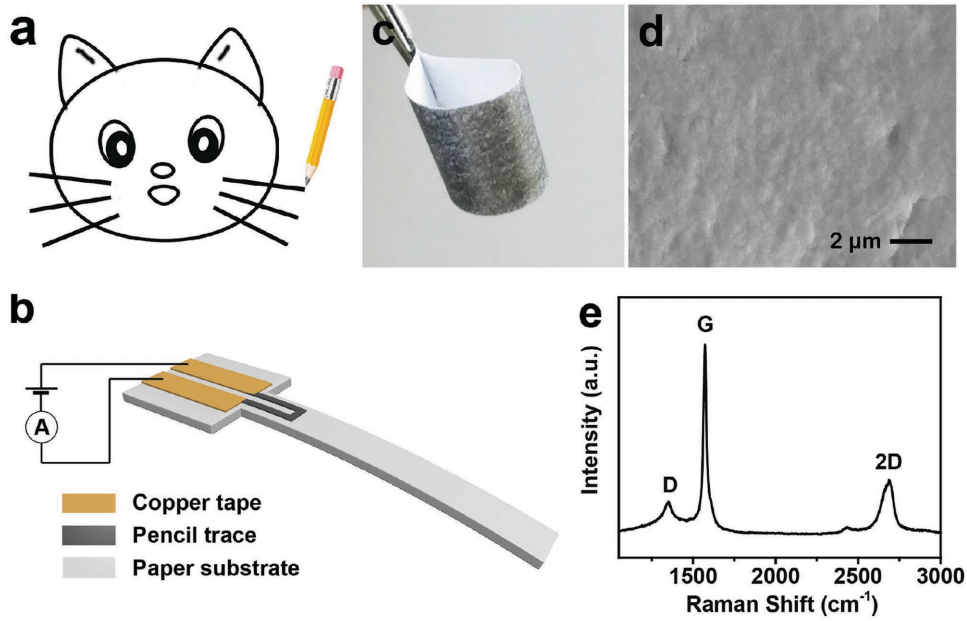

Figure 1. Materials and structure of pencil-drawn e-whisker. a) Schematic illustration of cat's whisker (vibrissal tactile perception). b) Device schematic of pencil-drawn e-whisker. c) Optical image of pencil trace on paper. d) SEM image of the pencil graphite on paper. e) Raman spectrum of the graphite pencil trace.

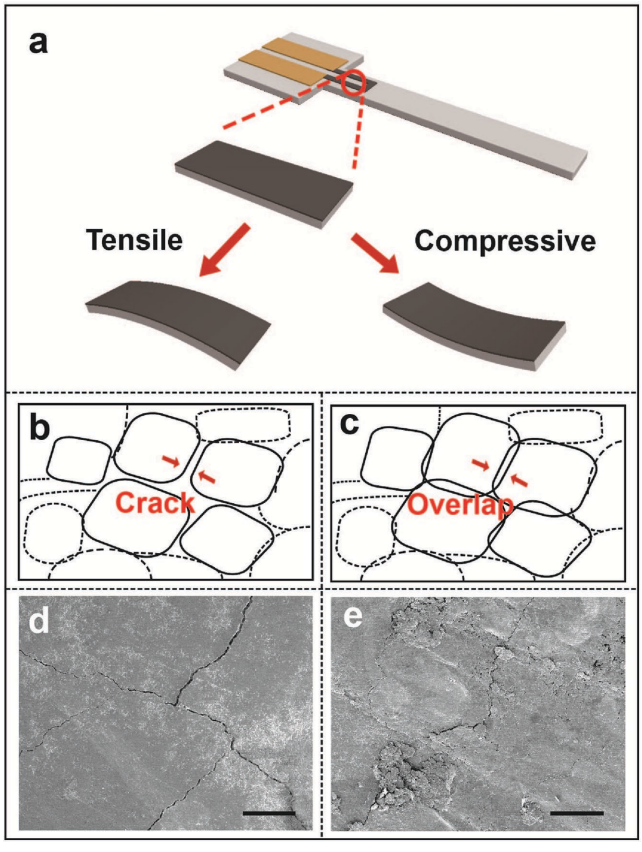

Figure 2. The sensing mechanism of pencil-drawn e-whisker. a) Schematic illustration of the graphite pencil trace of e-whisker when applied tensile or compressive strain. b,c) Schematics of the strain sensing mechanism. d,e) SEM images of the pencil trace when applied tensile or compressive strain, respectively. Scale bar: 20 μm.

approach to develop a novel facile fabricated e-whisker. The pencil-drawn e-whisker design is schematically presented (Figure S3a, Supporting Information), and the personalized pencil-drawn e-whisker arrays also illustrated (Figure S3b–e, Supporting Information). It should be noted that any common used paper can be collected for fabricating our e-whisker devices (see Figure S3c, Supporting Information), implying the great potential as a new environmental-friendly technology.

Figure 3a shows resistance changes of pencil-drawn e-whiskers that have a downward trend for strain sensing in compressive deflections, or upward for tensile ones. The gauge factor (GF), used to evaluate the strain sensing ability, is defined as GF = $(\Delta R/R_0)/\varepsilon$, where R_0 is the initial graphite resistance of the undeformed gauge, and ΔR is resistance change induced by external strain ε. In compressive bending, normalized resistance changes also indicate a linear relation with bending deflection downward from 0 to 13 mm, leading to a high GF of 18. Contrarily in tensile bending, we make deflection changing from 0 to 12 mm, normalized resistance changes exhibit a linear relation with the variation of bending deflection, resulting in a rather high GF of 34. Although the value of GF is much lower than carbon-nanotube sensor (GF = 600–1000)[23] or metal-crack sensor (GF = 2000),[24] it is higher than those previously reported mostly graphite strain sensors (GF = 4.1–20.7),[12,25,26] gold nanowires sensor (GF = 7.38),[27] all-elastomer strain sensor (GF = 29),[28] ZnO-fiber sensor (GF = 15.2),[29] and amorphous silicon (a-Si) or microcrystalline silicon (poly-Si) strain gauges (GF = 26, 31).[30,31]

In order to evaluate the mechanical robustness and sensing response performance, we conduct a pencil-drawn e-whisker curved with strains of ±0.37% (≈7 mm deflection) alternatively. The procedure of intentional e-whisker deflections, which is depicted in Figure 3b, demonstrates that the pencil-drawn e-whisker can function well and response fast. Importantly, this

© 2016 WILEY-VCH Verlag GmbH & Co. KGaA, Weinheim

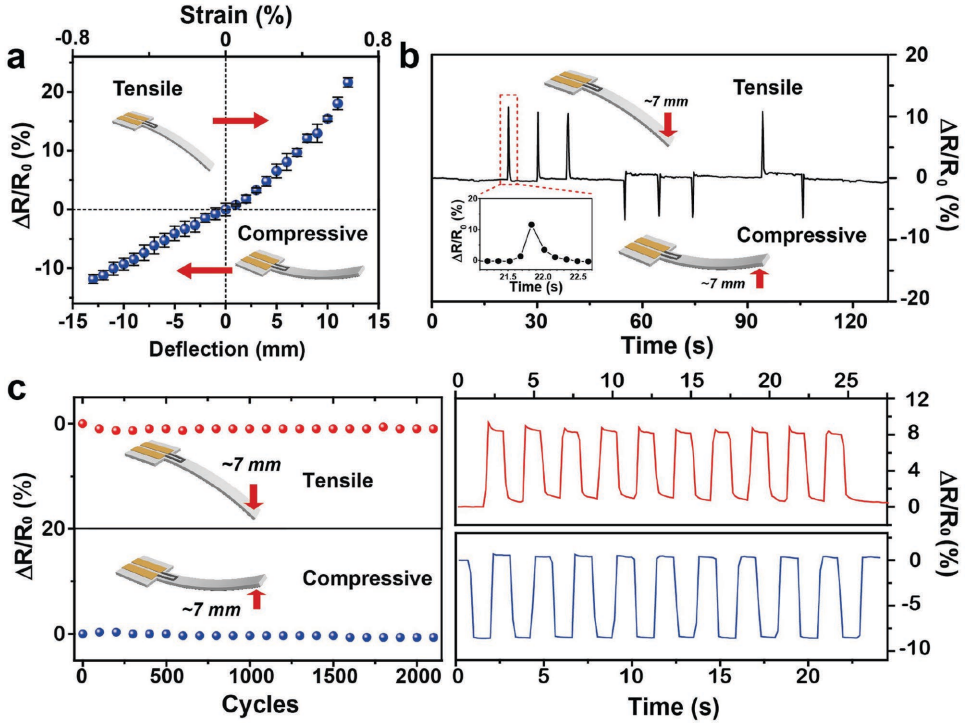

Figure 3. Strain sensing performance of pencil-drawn e-whisker. a) Normalized resistance change, $\Delta R/R_0$, as functions of deflection (bottom x-axis) and applied strain (top x-axis). b) Response performances of the pencil-drawn e-whisker when applied tensile and compressive strain by bending ≈7 mm, corresponding to ±0.37% strain. Inset exhibits that the temporal response of pencil-drawn e-whisker at tensile bending. c) Mechanical durability of pencil-drawn e-whisker by bending ≈7 mm for 2000 bending cycles. Ten cycles in tensile (top right) and compressive (bottom right) bending are shown after 2000 cycle.

e-whisker exhibits very rapid response time of 50 ms and recovery time of 76 ms (as shown in Figure S4, Supporting Information), which are much shorter than that of recently reported paper-based strain sensor.[13] We examine the mechanical durability (Figure 3c) of the pencil-drawn e-whisker by bending ≈7 mm both in tensile (top, red) and compressive (bottom, blue) modes. Normalized resistance changes do not exhibit any noticeable degradation after 2000 bending cycles. In addition, the detailed procedures of resistance change are observed in ten cycles of tension (Figure 3c, top right) and compression (Figure 3c, bottom right) after 2000-time bending, showing a superior mechanical robustness and reliability. Furthermore, the pencil-drawn e-whisker also performs excellently although relative humidity (RH) changes, according to the reversible resistance plots of Figure S5 of the Supporting Information.

Importantly, it should be noted that our personalized pencil-drawn e-whisker arrays have great potential applications in human-machine interfaces, health-monitoring systems, and encrypted information transmissions, as we proposed in **Figure 4**. We can communicate or interactive with machines through our pencil-drawn e-whisker arrays (Figure 4a). Moreover, a pencil-drawn device might be used to transmit information in the application of strain sensing, monitoring finger bending manners (Figure 4b). And temporal signals produced by finger bending are recorded effectively to represent the signs of "CAS" and "BINN" in Morse code, as depicted in Figure 4c.

Additionally, pencil-drawn e-whisker array would implement simultaneous detection of multiple contact points, and be capable of highly parallel and efficient 3D object contour extraction. Manifested from **Figure 5**, the spatial distribution upon touching an object, like mammalian whisker functions, is experimentally contoured by employing a nine pencil-drawn

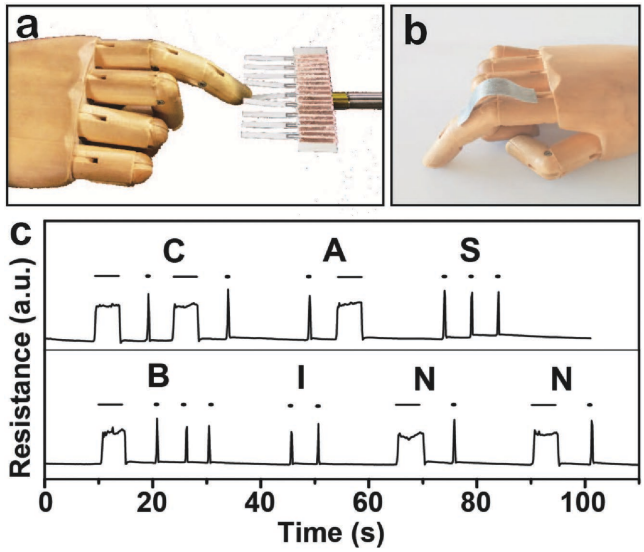

Figure 4. Pencil-drawn e-whisker as human-machine interface. a) Schematic image of pencil-drawn e-whisker array as human-machine interface. b) Schematic image of a pencil-drawn device in the application of strain sensing for monitoring human motion or transmitting information. c) Temporal signals produced by finger bending, representing the signs of "CAS" and "BINN" in Morse code.

© 2016 WILEY-VCH Verlag GmbH & Co. KGaA, Weinheim

ADVANCED ELECTRONIC MATERIALS
www.advelectronicmat.de

Materials Views
www.MaterialsViews.com

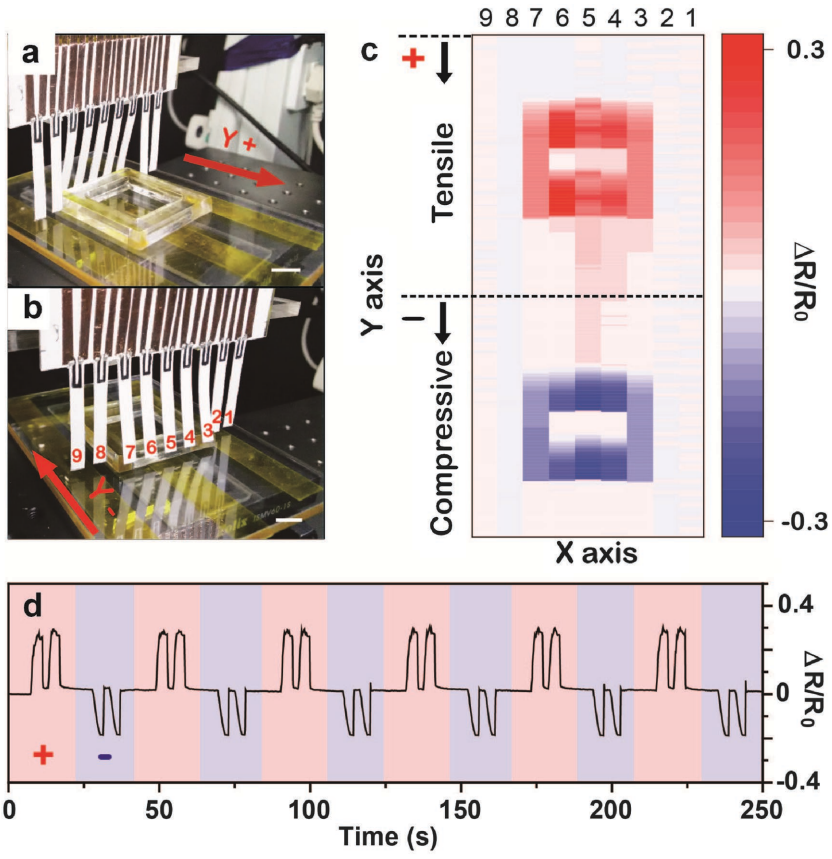

Figure 5. Spatial distribution mapping in tensile and compressive modes. a) Nine pencil-drawn e-whisker array (9-whisker-array) used for scanning an object "O" in forward direction (Y+), as tensile mode detection. Scale bar: 10 mm. b) 9-whisker-array used for scanning an object "O" in backward direction (Y–), as compressive mode detection. c) Pencil-drawn e-whisker array used for scanning an object "O" from Y+ to Y– direction consecutively. d) Normalized resistance change recording of No. 6 e-whisker in tensile and compressive modes for six consecutive sweeping cycles.

e-whisker array (9-whisker-array). The pencil-drawn e-whisker array can be conducted both in tensile and compressive modes (see Movie S1). An O-shaped object is scanned (scanning speed is 5 mm s^{-1}) using the 9-whisker-array in forward direction (Y+, presented in Figure 5a) and backward direction (Y–, see Figure 5b) in sequence. As described in Figure 5c, the distinct spatial distribution of "O" is mapped both in tensile and compressive modes, discriminating the object's shape. Scanning from Y+ direction (tensile mode), the normalized resistance change increases as the height of "O" augments, because different heights could induce deflection variations of pencil-drawn e-whiskers. By contrast, the normalized resistance change decreases as the height of "O" increases when scanned from Y– direction (compressive mode). In addition, changes in resistance of No. 6 e-whisker are real-time recording in tensile and compressive modes for six consecutive scanning cycles, indicating a favorable mechanical reliability for the spatial distribution mapping. Moreover, the scanning speeds are varied to evaluate the sensing performance of the pencil-drawn e-whisker array, as shown in Figure S6 of the Supporting Information. It can be found that resistances do not show any noticeable change at different scanning speed. And the e-whisker array functions well in a favorable stable condition, regardless of tensile and compressive deflections.

We also perform 3D spatial distribution mappings of the 9-whisker-array and detect two objects with different heights, as shown in **Figure 6**. An object in Figure 6a has a height of 5 mm, and another object in Figure 6b has three layers (thickness: 5 mm/2 mm/ 5 mm). The free ends of the 9-whisker-array are all about 2 mm away from the ground when it comes to move. Two pronounced 3D spatial imaging contours are extracted by sweeping the corresponding objects (as depicted in Figure 6c,d) in tensile mode. We can see from the 3D space mappings that color contrast contributes to differentiate the shapes of objects according to up and down steps of the e-whisker array scanning, and colors would get brighter with the height of touched objects increasing. The pencil-drawn e-whisker array is capable to obtain a comparable performance in 3D space mappings for the swept objects as the strain/temperature dual-mode e-whisker array did.[7] More importantly, it can identify the specific location, orientation and shape/size of touched objects, according to the resistance changes in tensile or compressive mode (see Figures 5 and 6). In addition, we can also reconstruct other objects' localization, orienting and shape by exploiting the simple and scalable personalized e-whisker array structures based on our pencil-on-paper approach.

In summary, bioinspired e-whisker arrays are demonstrated to adaptively sense/image strains with deflections in pencil-on-paper approach, which has the virtues of low-cost, easy fabrication, lightweight, disposable, as well as easily available, abundant, and environmental-friendly resources. The strain gauge of the fabricated pencil-drawn e-whisker exhibits a high GF of 34 and rapid response time of 50 ms, which is much faster than previously reports. The pencil-drawn e-whisker performances extremely well regardless of RH disturbance and has a superior mechanical robustness and reliability in durability tests. Inspired by mammalian vibrissal tactile ability, a 9-whisker-array is conducted to map 3D spatial distribution upon touching objects both in tensile and compressive modes, and used to reconstruct objects' localization, orienting, shape and size. This novel approach allows access to a wide range of potential applications in advanced robotics, artificial intelligence, human-machine interfaces, and health monitoring systems.

Experimental Section

Fabrication of the Pencil-Drawn e-Whisker: A 2B graphite pencil was used to draw uniform traces (Resistances: ≈30 kΩ) on the predesign-patterned A4 paper (≈300 μm thick, 180 g m^{-2}; patterns cut by a scissor). Silver paste was employed to form good electrical contacts between the pencil-trace and copper tapes.

© 2016 WILEY-VCH Verlag GmbH & Co. KGaA, Weinheim

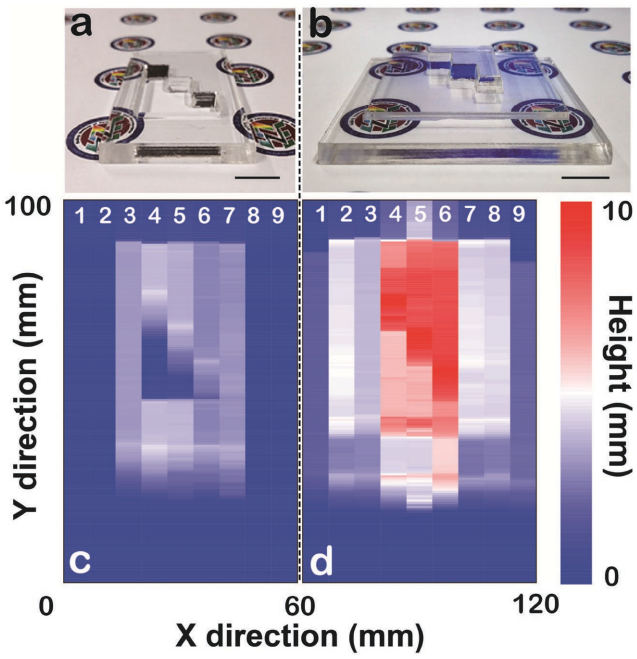

Figure 6. 3D spatial distribution mapping. a,b) Optical images of two objects for 3D spatial mapping. Scale bar: 10 mm. c,d) 3D spatial mapping contours produced by scanning two objects shown in (a) and (b), respectively.

Characterization: SEM images were conducted by Hitachi SU8020. Raman spectrum was conducted by a confocal Raman spectrometer (HORIBA LabRAM HR Evolution). Applied forces were calibrated by a high precision balance (Mettler Toledo, ME104, 0.1 mg). Resistances were recorded in real-time by a precision LCR meter (Agilent, E4980A) with custom LabVIEW programs. Currents were measured on a Keithley 4200 SC with a voltage bias of 1 V.

Supporting Information

Supporting Information is available from the Wiley Online Library or from the author.

Acknowledgements

Q.H. and H.L. contributed equally to this work. The authors are thankful for support from the "Thousand Talents" program of China for pioneering researchers and innovative teams and from the President Funding of the Chinese Academy of Sciences, National Natural Science Foundation of China (No. 51432005, 61405040, 61505010, and 51502018), and Beijing City Committee of Science and Technology (Z151100003315010).

Received: March 2, 2016
Revised: March 26, 2016
Published online:

[1] F. Ju, S. F. Ling, *Smart Mater. Struct.* **2014**, *23*, 125003.
[2] J. H. Solomon, M. J. Z. Hartmann, *IEEE T. Robot.* **2008**, *24*, 1157.
[3] P. Valdivia y Alvarado, V. Subramaniam, M. Triantafyllou, *Design of a bio-inspired whisker sensor for underwater applicaions*, presented at Sensors, 2012 IEEE, Taipei, 28–31 Oct., **2012**.
[4] T. Assaf, J. Rossiter, M. Pearson, *Contact sensing in a bio-inspired whisker driven by electroactive polymer artificial muscles*, presented at Sensors, 2013 IEEE, Baltimore, MD, 3–6 Nov., **2013**.
[5] T. Cagdas, L. J. Douglas, K. Farzad, *Bioinspir. Biomim.* **2015**, *10*, 046018.
[6] K. Takei, Z. Yu, M. Zheng, H. Ota, T. Takahashi, A. Javey, *Proc. Natl. Acad. Sci. USA* **2014**, *111*, 1703.
[7] S. Harada, W. Honda, T. Arie, S. Akita, K. Takei, *ACS Nano* **2014**, *8*, 3921.
[8] C. Pan, L. Dong, G. Zhu, S. Niu, R. Yu, Q. Yang, Y. Liu, Z. L. Wang, *Nat. Photonics* **2013**, *7*, 752.
[9] W. Wu, X. Wen, Z. L. Wang, *Science* **2013**, *340*, 952.
[10] R. Bao, C. Wang, L. Dong, R. Yu, K. Zhao, Z. L. Wang, C. Pan, *Adv. Funct. Mater.* **2015**, *25*, 2884.
[11] L. Pan, A. Chortos, G. Yu, Y. Wang, S. Isaacson, R. Allen, Y. Shi, R. Dauskardt, Z. Bao, *Nat. Commun.* **2014**, *5*, 3002.
[12] X. Liu, M. Mwangi, X. Li, M. O'Brien, G. M. Whitesides, *Lab Chip* **2011**, *11*, 2189.
[13] X. Liao, Q. Liao, X. Yan, Q. Liang, H. Si, M. Li, H. Wu, S. Cao, Y. Zhang, *Adv. Funct. Mater.* **2015**, *25*, 2395.
[14] D. J. Lipomi, M. Vosgueritchian, B. C. Tee, S. L. Hellstrom, J. A. Lee, C. H. Fox, Z. Bao, *Nat. Nanotechnol.* **2011**, *6*, 788.
[15] X. Zhao, Q. Hua, R. Yu, Y. Zhang, C. Pan, *Adv. Electron. Mater.* **2015**, *1*, 1500142.
[16] N. Kurra, G. U. Kulkarni, *Lab Chip* **2013**, *13*, 2866.
[17] C. W. Lin, Z. Zhao, J. Kim, J. Huang, *Sci. Rep.* **2014**, *4*, 3812.
[18] T. L. Ren, H. Tian, D. Xie, Y. Yang, *Sensors* **2012**, *12*, 6685.
[19] A. Russo, B. Y. Ahn, J. J. Adams, E. B. Duoss, J. T. Bernhard, J. A. Lewis, *Adv. Mater.* **2011**, *23*, 3426.
[20] W. J. Hyun, O. O. Park, B. D. Chin, *Adv. Mater.* **2013**, *25*, 4729.
[21] B. Yao, L. Yuan, X. Xiao, J. Zhang, Y. Qi, J. Zhou, J. Zhou, B. Hu, W. Chen, *Nano Energy* **2013**, *2*, 1071.
[22] Z. Li, H. Liu, C. Ouyang, W. H. Wei, X. Cui, T. J. Lu, P. M. Belinda, F. Li, F. Xu, *Adv. Funct. Mater.* **2016**, *26*, 165.
[23] J. Cao, Q. Wang, H. Dai, *Phys. Rev. Lett.* **2003**, *90*, 157601.
[24] D. Kang, P. V. Pikhitsa, Y. W. Choi, C. Lee, S. S. Shin, L. Piao, B. Park, K. Y. Suh, T. I. Kim, M. Choi, *Nature* **2014**, *516*, 222.
[25] X. Luo, D. D. L. Chung, *MRS Online Proceedings Library Archive* **1996**, p. 459.
[26] A. Bessonov, M. Kirikova, S. Haque, I. Gartseev, M. J. A. Bailey, *Sens. Actuators, A* **2014**, *206*, 75.
[27] S. Gong, W. Schwalb, Y. Wang, Y. Chen, Y. Tang, J. Si, B. Shirinzadeh, W. Cheng, *Nat. Commun.* **2014**, *5*, 3132.
[28] N. Lu, C. Lu, S. Yang, J. Rogers, *Adv. Funct. Mater.* **2012**, *22*, 4044.
[29] X. Liao, Q. Liao, Z. Zhang, X. Yan, Q. Liang, Q. Wang, M. Li, Y. Zhang, *Adv. Funct. Mater.* DOI: 10.1002/adfm.201505223.
[30] H. Gleskova, S. Wagner, W. Soboyejo, Z. Suo, *J. Appl. Phys.* **2002**, *92*, 6224.
[31] Y. Kervran, O. De Sagazan, S. Crand, N. Coulon, T. Mohammed-Brahim, O. Brel, *Sens. Actuators, A* **2015**, *236*, 273.

© 2016 WILEY-VCH Verlag GmbH & Co. KGaA, Weinheim